http://dx.doi.org/10.5935/0103-5053.20150238

J. Braz. Chem. Soc., Vol. 26, No. 12, 2418-2429, 2015.
Printed in Brazil - ©2015 Sociedade Brasileira de Química
0103 - 5053 $6.00+0.00

Review

Nonlinear Optical Properties and Femtosecond Laser Micromachining of Special Glasses

Juliana M. P. Almeida, Gustavo F. B. Almeida, Leonardo Boni and Cleber R. Mendonça*

Instituto de Física de São Carlos, Universidade de São Paulo, CP 369, 13560-970 São Carlos-SP, Brazil

Materials specially designed for photonics have been at the vanguard of chemistry, physics and materials science, driven by the development of new technologies. One particular class of materials investigated in this context are glasses, that in principle should exhibit high third order optical nonlinearities and fast response time, whose optical properties can be tailored by compositional changes, such as, for instance, the incorporation of metallic nanoparticles to explore plasmon resonances. Simultaneously to the development of novel materials, and motivated by the need of device miniaturization, direct laser writing by femtosecond pulses has been used to advanced processing of glasses. Such method allows fabricating high resolution three-dimensional optical devices, as well as to produce spatially localized metal nanoparticles. This review paper initially presents results on the nonlinear optical characterization of special glasses, in addition to progresses on the use of femtosecond laser micromachining for producing waveguides and spatially confined metal nanoparticles.

Keywords: nonlinear optics, femtosecond pulses, micromachining, special glasses

1. Introduction

Materials exhibiting high optical nonlinearities play a major role in the development of new technologies in optics and photonics. To enhance the performance of optical devices, a great deal of research has sought after materials with interesting nonlinear optical properties, including organic molecules, polymers, inorganic semiconductors and glasses. Specifically, glasses are of great interest because they can present high third order optical nonlinearities, especially those containing heavy metal elements.[1-3] Furthermore, their linear and nonlinear optical properties can be tailored by using distinct elements,[1,2,4] aiming at photonic devices for optical switching, optical limiters and infrared technologies, for example. At the same time, glasses containing metallic nanoparticles (NP) have also been developed with the objective to explore the enhancement of optical properties provided by the surface plasmon resonance (SPR).[5,6] Commonly, such glasses are prepared by the introduction of the desired metal ions into the glass matrix, followed by metal reduction that can be achieved by heat treatment.[2,3,7] Alternatively, femtosecond laser irradiation can also be used to promote the metal reduction and subsequent nanoparticle formation.[7]

*e-mail: crmendon@if.sc.usp.br

In parallel to the development of novel materials and motivated by the miniaturization of devices required for technological applications,[8] femtosecond laser micromachining has been explored for the fabrication of micro/nano structures in glasses. Such method allows high resolution and the ability to structure materials in 3D, and can be used to ablate or modify structural properties of materials. The use of femtosecond laser pulses for micromachining transparent materials has been employed to fabricate several optical devices, such as, resonators, couplers, splitters, data storage and waveguides, most of them in standard optical glasses.[9,10] Since the first demonstrations of waveguides fabrication in glasses using femtosecond laser micromachining,[11,12] several works have been done to perfect it through the optimization of laser parameters and irradiation conditions.[13,14] More recently, however, femtosecond laser pulses have also been used to promote photoreduction of ions within the glass and subsequent production of metal nanoparticles through nucleation and growth.[15,16]

In this context, this paper describes some results that our and other research groups have obtained on the nonlinear optical properties of special glasses, with emphasis to the nonlinear refraction and absorption. Additionally, achievements on the use femtosecond laser pulses to micromachine such glasses, with special attention to the

fabrication of waveguides and the production of spatially confined metal nanoparticles are also described.

2. Experimental Methods

2.1. Nonlinear optical characterization

To characterize the nonlinear optical properties of glasses, one of the most widely used approaches is the Z-scan technique, originally developed by Sheikbahae *et al.*[17] Essentially, this method monitors changes in the nonlinear transmittance as the sample is scanned through the Z-axis, which contains a focused Gaussian laser beam. One of its advantages is allowing obtaining the nonlinear refraction and the nonlinear absorption by placing (closed-aperture) or removing (open-aperture) an aperture in the far field, respectively. As excitation sources for Z-scan experiments, lasers pulses with duration from nano to femtoseconds and distinct repetition rates and wavelengths can be employed. However, most of the recent studies in glasses have been obtained using femtosecond laser pulses and low repetition rate (kHz), usually delivered by Ti:sapphire chirped pulse amplified systems. Furthermore, in order to obtain the spectral response of the nonlinear refraction and absorption, optical parametric amplifiers (OPA) pumped by the Ti:sapphire laser have been used, allowing excitation source tuning from 450 up to 2000 nm, typically. Alternatively, it has also been shown that white-light continuum (WLC), produced by focusing infrared fs-pulses on water or sapphire, can also be used to determine the spectrum of optical nonlinearities using the so called WLC Z-scan technique.[18]

For determining electronic nonlinear refraction and multi-photon nonlinear absorption, in general, Z-scan measurements are carried out with intensities in the order of 100 GW cm^{-2}. For a refractive nonlinearity, the light field induces an intensity dependent refraction, $n = n_0 + n_2 I$, where I is the laser beam irradiance, n_0 is the linear index of refraction and n_2 is the nonlinear index of refraction associated with the electronic response, which can be obtained through the closed aperture Z-scan. Conversely, for a sample presenting multi-photon absorption, specifically two-photon absorption (2PA), the light field creates an intensity dependent absorption, $\alpha = \alpha_0 + \beta I$, in which α_0 is the linear absorption coefficient, and β is the 2PA coefficient, determined by the open-aperture Z-scan.

The dynamics (response time) of optical processes in glasses are usually determined using pump-probe methods. In such type of experiments, the sample is excited by fs-pulses focused into the sample (pump), with the pulse energy below the damage threshold. The time-resolved optically induced response is measured with a second pulse (probe) time delayed in respect to the pump.[19,20] Ti:sapphire laser systems, as well as OPAs are generally used as excitation sources. Most of the ultrafast dynamics pump-probe experiments are performed in two distinct configurations; (*i*) optical Kerr gate (OKG) and (*ii*) excited state absorption (ESA).

For the OKG, the laser beam is split into pump (strong) and probe (weak-a few percent of the pump) beams. The probe beam polarization is set at 45º with respect to the pump beam. Pump and probe beams were focused and spatially overlapped into the sample. An analyzer, whose transmission axes is crossed with respected to the first one, is placed after the sample and before the photodetector. The light transmittance through the analyzer, due to the transient birefringence induced in the sample by the pump, is monitored as a function of the time-delay between pump and probe.

In the ESA configuration, transient transmittance measurements can be performed using as a probe beam either a discrete wavelength (portion of the pump or a OPA beam) or a WLC probe, usually generate by using a small fraction of the pump beam in a sapphire window. The pump induced transmittance changes are measured as a function of the time delay between pump and probe pulses, carefully varied by a computer controlled translation stage.

2.2. Linear optical and structural characterization

After the glass sample preparation and prior to its nonlinear optical studies, they are usually characterized by X-ray diffraction (XRD), Raman spectroscopy and differential scanning calorimetry (DSC). For samples presenting nanoparticles, its presence and nature are usually checked by high resolution transmission electron microscopy (HR-TEM) and selective area electron diffraction (SAED). Linear absorption (UV-Vis) and fluorescence spectra measurements are usually carried out as complimentary results to the nonlinear optical characterization.

2.3. Femtosecond laser micromachining in glasses

Laser micromachining is performed by focusing the femtosecond laser into the sample volume or surface, while the sample is translated or the laser beam is scanned. The intensity level achieved by ultrashort pulses at the focus is usually high enough to cause nonlinear interaction, which can lead to structural changes, photo-reduction, degradation or ablation of the material. The nonlinear nature of the light-mater interaction confines the process to the vicinity of the focal volume.

From the experimental point of view, femtosecond laser (fs-laser) micromachining can be accomplished by optical systems that three-dimensionally scan the sample stage, or by setups in which scanning mirrors are responsible for the two-dimensional scanning of the beam, while the z axis movement is carried out by a translation stage. Figure 1 displays a schematic representation of the micromachining setup using the translation stages. The laser beam is focused into the sample by microscope objectives with different numerical apertures (NA). Basically, the NA determines the width of the focal volume and, consequently, the micromachining feature size. Moreover, the NA also influences the geometry of the structures; while small NAs produce asymmetric structures, high NAs allow producing spherically symmetric features. The sample is placed on a computer-controlled x-y-z stage that moves the sample with a constant speed in relation to the objective lens that remains fixed. The fabrication process can be accompanied in real time using a charge-coupled device (CCD) camera.

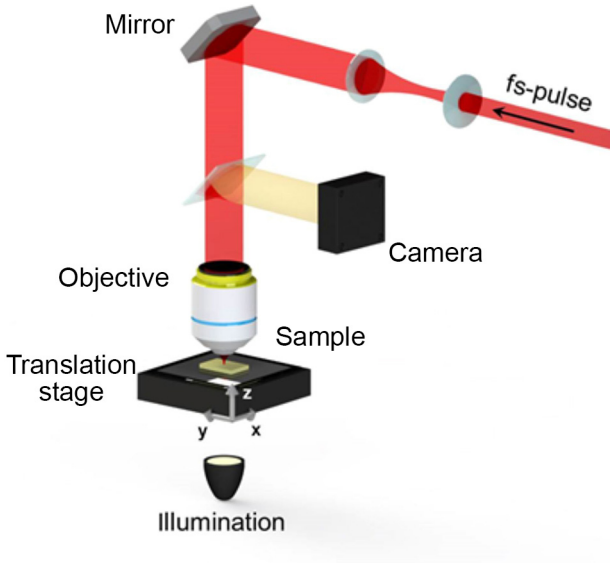

Figure 1. Illustration of the experimental setup used for the fs-laser micromachining.

In general, fs-laser micromaching in glasses can be achieved with pulse energies on the order of nanojoules, which can be obtained through laser oscillators (not amplified systems). In this case, the time interval between consecutive pulses is smaller than the heat diffusion time, giving an accumulative nature to the micromachining process.[9,21] Thus, one of the most employed excitation sources for fs-laser micromachining in glasses are Ti:sapphire laser oscillators operating at an wavelength of approximately 800 nm and with repetition rate of MHz. Naturally, other wavelengths and repetition rates can also be used. However, when laser systems operating at kHz repetition rate are used the micromachining process becomes repetitive, as opposed to the cumulative nature obtained when oscillators are employed.[9] The micromachined samples are usually analyzed by optical microscopy, atomic force microscopy, scanning electron microscopy and standard spectroscopic tools (UV-Vis, fluorescence and Raman).

3. Nonlinear Optical Spectroscopy in Glasses

Nonlinear optical spectroscopy in glasses have been extensively studied at the last decades due to their vast application in devices, such as all-optical switches.[22] The potential of these optical glasses reside on the possibility to operate devices at speeds and bandwidths greater than electronics. Optical glasses present high transparency in a large wavelength range. Additionally, the response times of the nonlinear effects are, in most cases, related to parametric effects, whose origin is purely electronic.[23]

In this research area, several optical glasses have been studied. For example, Friberg *et al.*[22] measured nonlinear index coefficients of several glasses using degenerate four-wave-mixing[24] at 1.06 μm, in order to obtain the response time of optical glasses to be used as all-optical switches. By measuring the relative magnitudes of the fast and slow nonlinearities of the samples, they were able to quantify switching power and thermal index change, which are related, respectively, to nonlinear refraction index (n_2) and change in the linear refraction index with the local temperature (dn/dT). By observing both effects on glasses, they defined a new figure of merit (FOM) for nonlinear optical materials used for ultrafast waveguide switching devices, in order to address thermal effect problems and fast-time-response requirements. The greatest result observed on SF-59 glass was a FOM about 10 times higher than the one to semiconductor doped glasses and 100 times higher when compare to GaAs and GaAs/GaAlAs. Even though n_2 is about 100 times smaller for SF-59 than for GaAs, the FOM increased because SF-59 presents a very small linear absorption and a small change in the linear refractive index due to the induced local temperature. This work was prominent to define a way to look for new materials for photonics that need to present a combination of larger n_2, smaller absorption and fast response times.

Approximately one year later, Hall *et al.*[25] demonstrated that chalcogenide glasses, in specific glasses with heavy metals such as lead and bismuth, which present linear refractive index (n_0) higher than SF's glasses, also present higher n_2. In that work,[25] they demonstrated a correlation between heavy metal content and nonlinear susceptibility

($\chi^{(3)}$), and predicted an upper limit to $\chi^{(3)}$ in this type of material. They observed an enhancement of a factor of 3 for lead-bismuth-gallate when compared with glasses reported elsewhere.

Smolorz *et al.*[6] also studied chalcogenide and heavy-metal oxide glasses using the Z-scan technique. They described a monotonically increase of the nonlinear index of refraction as the excitation wavelength approaches the absorption edge of the sample. This effect was ascribed to a resonance enhancement caused by two-photon absorption on the material. As mentioned on that work, sometimes this effect is not desired on glasses because the increased refractive nonlinearity comes together with nonlinear absorption. Once nonlinear absorption is present, thermal effects, which have long relaxation times, may also appear, which is not desired for all-optical switches.

Chalcogenide glasses have been an important topic of study in nonlinear optics. In 2003, Zakery *et al.*[26] elaborated an important review on this subject. They reviewed different works with different experimental techniques to compare the magnitude of n_2 as a function of the nonlinear absorption and band gap energy for many chalcogenide glasses. An important information described on that work was that at near half-gap, chalcogenide glasses, such as As_2S_3, $GeAsS_e$, $Ge_{25}Se_{65}Te_{10}$, a maximum FOM is desirable for all-optical switching because it permits the design of an efficient switch with a large nonlinearity. The FOM increases near $\hbar\omega/E_{gap}$ ca. 0.45 when the absorption edge is not completely sharp. They described a remarkable value of FOM of about 11 for $As_{40}Se_{60}$. In special, this optical glass displays a nonlinear refractive index higher and two-photon absorption lower than other glasses cited on the review.

In parallel to these works, Vogel *et al.*[27] studied nonlinear optical effects on silicate glasses, observing which changes in structural and optical properties mainly modified the nonlinear optical response. Studying an optical glass system composed by different proportion of four components; TiO_2, Nb_2O_5, Na_2O and SiO_2, they described a dependence on the linear and nonlinear refractive index with the composition. Both, linear and nonlinear refractive indices were observed to increase when a combination of Ti and Nb cations were present in the glass composition, in comparison with the matrix with only Nd. However, the composition with Ti only presented the highest increment for n_2. Additionally and curiously, the main report on that work was to observe that the nonlinear refraction was much more sensitive to distinct cation than n_0.

The FOM defined by Friberg *et al.*[22] has been used from that time until nowadays. Many works are employing this definition to classify new optical glasses that could have potential application on optical switches. In 1990, Lines[28] elaborated a comparative study in oxide glasses for fast photonic switching. He described general restrictions for researchers when looking for new optical glasses aiming at all-optical switching. Some of the restrictions are related to a range of operating wavelengths of the optical switches. First, the frequency of the light (ω) needs to be lower than the lower limit determined by the nonlinear absorption of the material ($E_g/2$). It will avoid two-photon absorption process. Second, the frequency needs to be higher than the overall frequency (Ω) of the optical phonon modes present on the material. Based on these points, the energy range of interest for all-optical switches was defined as $10\hbar\Omega \lesssim \hbar\omega \lesssim E_g/2$. Throughout this range, n_2 is almost completely dominated by its electronic component in most of cases. Using his definition and elaborating a figure of merit, he identified that the empty d-band transition metal oxides gallates and tellurites glasses were the most promising candidates for operation on the telecommunication region. The relation with unfilled or empty d shells such as Ti^{4+} that contributes more strongly to the nonlinear polarizabilites was also confirmed by Sabadel *et al.*[29] Another interesting feature pointed out is that the largest nonlinear responses are generated by the highest valence metal cations or by the maximum p-d orbital overlap.[29]

Third-order nonlinear spectra and optical limiting of lead oxifluoroborate glasses[20] have been studied from 500 nm up to 1600 nm using femtosecond Z-scan technique. In that work, an increase and a small red shift on the two-photon absorption spectrum was described and related to a reduction of the band-gap energy of the glasses due to the amount of PbO added to the glass (see Figure 2a). Additionally, it was reported an enhancement of n_2 as a function of the cation concentration in the glass matrix. By increasing the percentage (x) of xPbO of x = 25, 35 and 50% and, consequently, decreasing the percentage of $(50 - x)PbF_2$ led to an increase in the nonlinear refractive index from 14 to 25 times higher than the value reported for fused silica.[30] In Figure 2b, a constant value as a function of the wavelength for n_2 of approximately $4.9 \times 10^{-19}\,m^2W^{-1}$ was observed for the sample containing 50% of PbO.

Almeida *et al.*[31] have studied another interesting class of glasses; borate glasses doped with transition metals. In that work, by using Z-scan they quantified the nonlinear refraction index on the wavelength range from 600 nm up to 1500 nm. A value of about twice of the fused silica[30] was determined. They observed that the nonlinear index of refraction was mainly defined by the matrix composition and that the addition of transition metals with a small concentration, of about 0.1 mol%, did not modified significantly the n_2 values on the range studied. Even

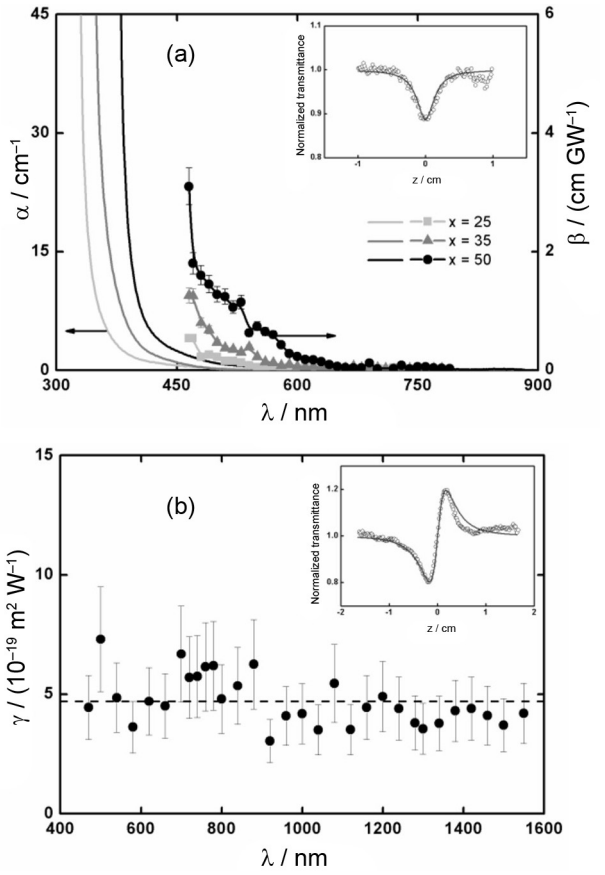

Figure 2. (a) Linear (solid line) and nonlinear (line + symbols) absorption spectra of $50BO_{1.5}$·(50 – x)PbF_2·xPbO glasses (x = 25, 35 and 50 cationic %); (b) values of the nonlinear refractive index as a function of wavelength for the glass with x = 50 cationic %. The insets show the (a) open and (b) closed aperture Z-scan signature for the x = 50 sample at 700 nm (adapted from reference 20).

though the linear optical properties were significantly changed, the nonlinear optical properties were kept the same. Waveguides and its application were also studied on that work for borate glasses and optical losses have been quantified.

As it can be seen, many optical glasses have been studied to be employed as all-optical switches, waveguides and so on. Not less important in this field is the study on the incorporation of nanoparticles on the glass matrix, in order to observe changes in the linear and nonlinear optical properties. Uchida *et al.*[32] have studied optical nonlinearities in glasses as a function of high concentration of small metal particles (between 5 and 50 nm radius), specifically copper and silver nanoparticles. The interesting information reported on that work was that nonlinear optical process increases as a function of the nanoparticles concentration incorporated on the glass matrix. Additionally, they observed that the nonlinear effect also increases with the size of the nanoparticles, achieving saturation for higher nanoparticles radius.

In the same direction, Falcão-Filho *et al.*[33] have studied third-order nonlinearities of transparent glass ceramics containing sodium niobate nanocrystals at two specific wavelengths, by using Z-scan and optical Kerr-gate. They observed two interesting opposite behaviors for the nonlinear optical process on this class of glasses; at 1064 nm a positive n_2 that increases with the nanocrystals concentration (filling factor) was observed. However, at 532 nm the n_2 also increased in module as the concentration of nanocrystals increases, but it presentes a negative value due to the proximity of the photon energy with the band gap energy.

De Boni *et al.*[34] have studied third-order nonlinear effects on lead-germanium oxide glasses containing small concentration of silver nanoparticles. By using femtosecond Z-scan and white-light Z-scan[18] techniques, they obtained the nonlinear refractive index and nonlinear absorption coefficient spectra. The interesting behavior noticed on that work is that there is not dependence of n_2 with small quantities of nanoparticles (less than 2%). The n_2 exhibits the same value and signal for the nonlinear refractive index, even when the photon energy approaches the band-gap energy. However, the nonlinear optical absorption shows a strong dependence on the nanoparticles content. In this case, the two-photon absorption effect, close to the plasmonic band of the nanoparticle, was significantly increased when compared with the glass without nanoparticles. Additionally, the authors observed an inversion of the nonlinear absorption effect when the photon energy was in resonance with plasmonic band. Saturable absorption instead of two-photon absorption was confirmed at the nanoparticles plasmon band.

Glasses containing heavy metal oxides, such as PbO, WO_3, Bi_2O_3 and Sb_2O_3[6] were the subject of research because their nonlinear optical effects can be enhanced by using the proper concentration of the hyperpolarizable elements. Heavy metal oxide glass containing metallic copper nanoparticles were also studied in order to observe the enhancement effect on the nonlinear refractive index due to the amount of the nanoparticles formed on the glass. Manzani *et al.*[35] employed femtosecond and white-light Z-scan techniques, combined with optical Kerr-gate and transient transmittance (pump-probe) experiments to reveal the nonlinear absorption and refraction, as well as their relaxation times. Manzani *et al.*[35] observed that the copper nanoparticle formation on tungsten lead-pyrophosphate glasses increases the third-order nonlinear process. They observed an enhancement of about three times when compared with the glass without nanoparticle for the region close to the copper plasmonic band (ca. 800 nm).[35]

An interesting point observed was that the nonlinear absorption changes its signal from positive to negative with the presence of the Cu^0 nanoparticles.[35] This effect is very similar to the one observed by De Boni *et al*.[34] indicating that inside the plasmonic band a saturable absorption prevails. According to Manzani *et al*.,[35] the enhancement of the n_2 with the presence of Cu^0 nanoparticles is explained by the long relaxation time (ca. 2.3 ps) measured in the transient absorption experiment at 560 nm. This time is related to the energy exchange from the excited electron of the nanoparticles to the matrix glass (electron-phonon interaction). This relaxation time was not observed for 780 nm, excitation wavelength outside of the nanoparticles plasmon band. For this wavelength, only Cu^{2+} was excited, displaying a response time shorter than 200 fs.

Another interesting work in glasses with nanoparticles was reported on heavy metal oxide glasses containing gold nanoparticles.[36] By using femtosecond Z-scan and optical Kerr-gate, the authors observed that these glasses present an average value for n_2 of about 1.8×10^{-19} $m^2 W^{-1}$ from 500 nm up to 1500 nm, one order of magnitude greater than fused silica. In Figure 3 it is possible to observe changes in the signal of the nonlinear absorption caused by the presence of Au nanoparticles. Figure 3a displays a decrease on the normalized transmittance due to a two-photon absorption effect when the energy of the photon is close to the band-gap edge. With the presence of the Au nanoparticles, Figure 3b, both effects, two-photon absorption and saturable absorption, were observed simultaneously for the same excitation wavelength (500 nm, inside of the plasmonic band). The interesting information described by Almeida *et al*.[36] is that the nonlinear absorption coefficient magnitude related to the two-photon absorption was not changed by the presence of the nanoparticles. However, the presence of Au nanoparticles added a new absorption effect on the glass matrix.

As it can be seen, third-order nonlinear optical effects have been studied in a vast classes of glasses with or without nanoparticles. The presence of nanoparticles tends to enhance the nonlinear refractive index until a saturation point, determined by the nanoparticles concentration. Additionally, nanoparticles have also enhanced nonlinear absorption (most of the time two-photon absorption) effects only in the region close to the plasmonic band. Moreover, inside the plasmon band a new effect on the nonlinear absorption of the optical glasses containing nanoparticles were added, creating a region in which nonlinear absorption can be controlled by the concentration of the nanoparticles.

Qu *et al*.[37] also demonstrated nonlinear absorption in glasses containing gold nanoparticles, induced by femtosecond pulses. Irradiating glasses containing Au nanoparticles with different intensities, the authors observed a decrease in the plasmonic absorption band intensity as a function of the average intensity. Furthermore, using nanosecond pulses at 523 nm they observed that the saturable absorption also decreases proportionally to the Au plasmon band decrease. At high irradiation intensity, in which the plasmon band is not more visualized at 530 nm, only reverse saturable absorption was measured, indicating that the control of nanoparticles concentration and plasmon band position are useful to tune nonlinear effects.[36]

4. Fs-laser Written Waveguides in Glasses

The origin of 3D waveguides in glass is related to studies on laser-induced breakdown in dielectrics. The damage caused by laser-matter interaction has been investigated

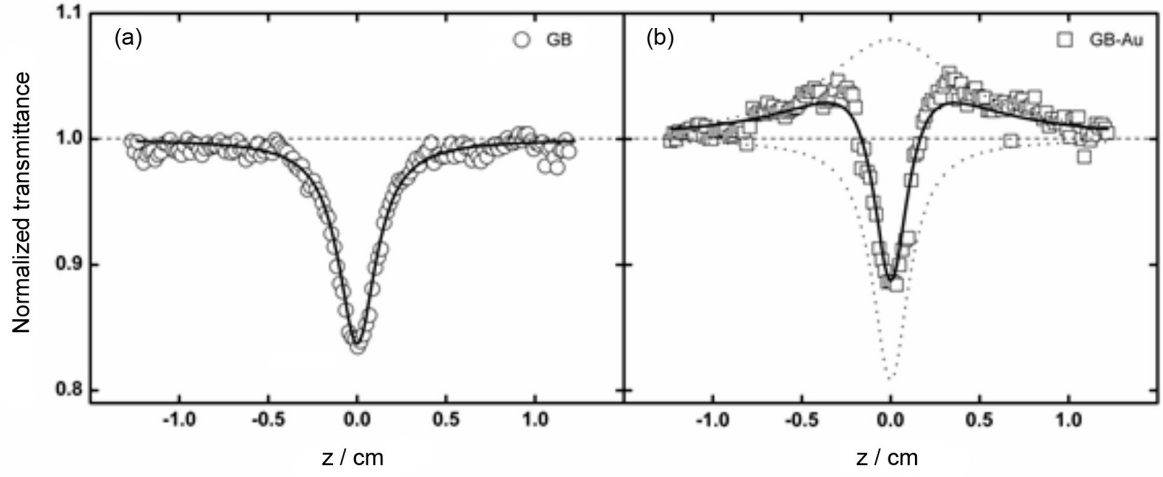

Figure 3. Open aperture Z-scan signature at 500 nm for GB and GB-Au. Open symbols represent the experimental results, while solid lines are the fitting curves. In the GB-Au, the dotted lines correspond to the individual theoretical curves for SA (normalized transmittance higher than one) and 2PA (normalized transmittance lower than one), while the solid curve represents the sum of both processes (adapted from reference 20).

since the laser development in 1960.[38] Nevertheless, the possibility to fabricate optical waveguides was reported about three decades later, when femtosecond lasers became available at research laboratories. Investigating the damage produced by fs-pulses tightly focused inside fused silica, Hirao and co-workers[11] observed a local change in the refractive index, Δn, of approximately 0.015. The nature of this Δn was discussed considering effects on the glass network resulting from localized melting or defects formation, as peroxy radicals, Si E'and nonbridging oxygen hole centers. Moreover, multiphoton processes were associated with laser-induced damage.[11] In the following year, the functionality of those damage lines for waveguide was demonstrated and the role of fs-laser became clearer.[12] Due to the high intensity in the focal volume, multiphoton absorption occurs, confining material ionization and plasma formation in the focused region inside the glass. The further interactions can lead to a local heating, and therefore structural densification during cooling and increase of the refractive index.[11,39] The process of laser-induced modification in glass is illustrated in Figure 4, in which multiphoton ionization, confined in the focal volume, results in structure densification and changes in the refractive index.[14,40]

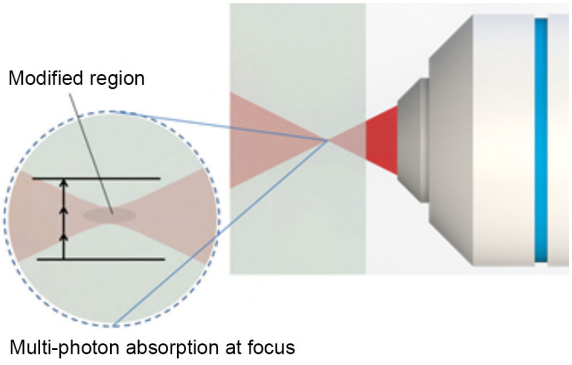

Figure 4. Representation of laser-induced damage in glass due to nonlinear optical interaction within the focal volume.

The guided modes are mainly determined by the shape, size and Δn of the waveguide, which can be controlled by the writing conditions, including the average power and repetition rate of the fs-laser, as well as sample scan speed and numerical aperture of the objective.[12,41] Moreover, the direction of sample movement defines the waveguide geometry. Elliptical or roughly cylindrical cross sections are obtained when the sample is translated transversally or longitudinally to the laser beam, respectively.[11] Although cylindrical waveguides favor the light coupling and guiding, their length is limited by the work distance of the employed objective, usually shorter than 10 mm for NA > 0.25. Thus, at the beginning of 20th century one of the first issues to be solved dealt with the asymmetry of the waveguides when produced by transversal writing. Such asymmetry follows the beam intensity profile where nonlinear interactions take place. Therefore, it is feasible that the waveguide cross-section be equivalent to the confocal parameter ($b = 2\pi w_0^2/\lambda$) along the beam propagation direction and correspondent to the beam diameter $2w_0$ when seen perpendicularly to it. In order to control the beam diameter without affecting the focal length, Osellame *et al.*[42] developed the astigmatic beam-shaping technique, in which a telescope with cylindrical lenses is employed so that the size and symmetry of the waveguide can be adjusted. A modification on the experimental setup became the micromachining of cylindrical waveguides simpler. Similar beam shaping can be achieved by using a slit, positioned before the objective lens and oriented parallel to the sample translation direction.[43,44] Figure 5a shows a nonfunctional waveguide and its elliptical cross-section, produced by a fs-laser (800 nm, 120 fs, 1 kHz) in a phosphate glass, using a 20× (NA = 0.46) and scan speed of 40 μm s^{-1} without slit. Using a slit of 500 μm, cylindrical waveguide is performed, as shown in Figure 5b, enabling the light confinement. To obtain a waveguide with symmetric profile the ratio between the beam waist at perpendicular directions to the laser propagation must be $\frac{w_y}{w_x} = \frac{NA}{n}\sqrt{\ln 2/3}$ at the objective entrance, where n is the refractive index and x is the waveguide axis, according to the description.[43]

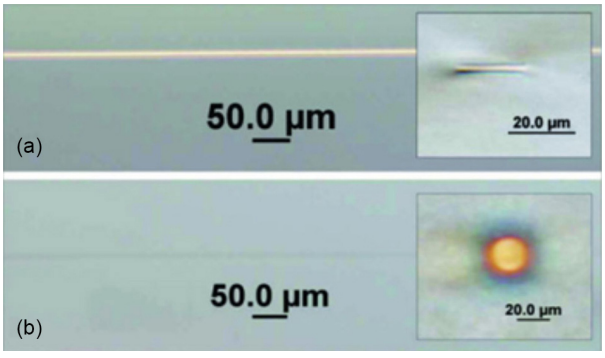

Figure 5. Differential interference contrast microscopy showing waveguides and their cross-sections, when micromachined (a) without and (b) with a slit before the objective lens.[43] Reprinted with permission from (Ams *et al.*,[43] 2005). Copyright (2015), The Optical Society (OSA).

Other drawback was related to the processing speed of those waveguides. The amplified laser systems employed so far own repetition rate of the order of kHz, which restricted the increase of the processing rate. Thus, the development of long cavity Ti:sapphire oscillator provided fs-pulses at MHz rate with enough energy per pulse for such task. Although the pulse energy decreased from μJ to nJ, the time interval between two consecutive pulses rises typically from ms to

ns, bringing not only faster laser scan speed, but also new issues concerning the heating accumulation effect. Given that the heat diffusion time out of the focal volume of a high numerical aperture lenses is about 1 μs, there is no enough time for the irradiated region cools down, resulting on the increase of the temperature and consequently melting/material modification in a dimension much larger than the focal volume.[13] Structures composed by concentric rings are commonly seen when fs-lasers with repetition rate of MHz are used, as illustrated on the top-view microscope image of Figure 6. The inner ring represents the region achieved by laser pulses, where nonlinear effects initiated by multiphoton absorption and followed by multiphoton- and avalanche ionization take place.[45] Part of the energy absorbed by the electrons is transferred to the lattice, and the central region acts as a heat source outwards the focal volume. The local temperature can achieve values as high as several thousand ºC. Then, the melted glass resolidifies according to the temperature and pressure gradients, leaving stress-stain zone that affects the inner region and giving rise the outer rings.[46,47] The magnitude of the heat affected zone, and therefore the waveguide size, depends on the number of laser pulses, thermal diffusion coefficient and the material's optical band gap, which defines the nonlinear interactions. Furthermore, in general, 200 kHz can be defined as the onset of repetition rate for heat accumulation effects generated by laser in glass. Because of its high band gap energy and melting temperature, pure fused silica is a particular case, requiring wavelength closer to the band gap and greater pulse energy and repetition rate.[46] Nevertheless, waveguides can be micromachined in fused silica by using fs-lasers of low repetition rate (1 kHz), in which the change of refractive index is controlled by the laser scan speed.[41]

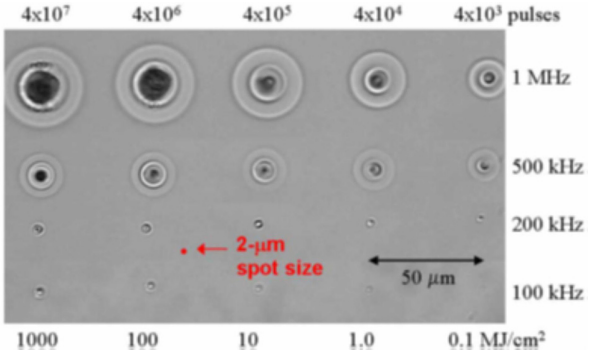

Figure 6. Dependence of laser-induced damage in a borosilicate glass (AF45) with the repetition rate, number of pulses and fluence of a 1045 nm femtosecond laser. Beam direction is normal to the image plane.[46] Reprinted with permission from (Eaton *et al*.,[46] 2005). Copyright (2015), The Optical Society (OSA).

In this sense, the choice of MHz or kHz laser systems substantially affects the resulting photo-written structure. If thermal effects are adverse, as in the obtainment of sub-micrometric structures, low repetition rate are appropriate, whereas high repetition rate lasers can play as a heat source, being beneficial for the reduction of waveguide loss, induced crystallization and ionic diffusion.[46,48] Encompassing diffusion and crystallization with nonlinear optical processes caused by fs-laser pulses, it has been possible to control the formation of metallic nanoparticles three-dimensionally at micrometer scale.[19,49,50] There are several interests on metallic nanoparticles in glass, as discussed in nonlinear optical spectroscopy section, however its control through fs-laser micromachining might be an important advance towards the development of metamaterials for all-optical devices. Both, low and high repetition rate lasers enable the space-selective formation of metallic NPs.[19,51,52] That is because the nucleation process is a consequence of the nonlinear interactions, such as multiphoton ionization that promotes electrons from valence to conduction band, giving rise to photoreduction reactions. Metallic ions present in the glass matrix, like Ag^{+}, Au^{3+} and Cu^{2+}, trap the free electrons to form neutral atoms. Once nonlinear optical processes promoted the nucleation, a heating source is necessary to promote the diffusion and aggregation of those metallic atoms. Therefore, space-selective formation of metallic NPs is achieved using only direct laser writing when MHz fs-laser is applied, while an additional annealing, usually carried on temperatures close to the glass transition, is required for the case of low repetition rate.

A practical way to check if the precipitation of metallic nanoparticles occurred is through the absorption spectrum, which must present the surface plasmon resonance at visible region. Figure 7 shows the extinction spectra of an Au_2O_3 doped silicate glass after the irradiation using three different intensities (from a 800 nm, 120 fs, 1 kHz laser) and subsequently annealing. The effect of irradiation with intensities of 6.5×10^{13}, 2.3×10^{14} and 5.0×10^{16} W cm^{-2} plus heating, resulted in the formation of bands centered at 568, 532 and 422 nm, respectively. The bands seen on spectra Figures 7a and 7b are due to surface plasmon resonance (SPR) of Au nanoparticles, whereas the spectrum in Figure 7c has been assigned to undecagold compounds with small Au clusters.[49] The blue shift on the SPR bands with the increase of light intensity represents a decrease on the average size of Au nanoparticles, suggesting that higher intensities improves the formation of neutral Au^0 atoms per unit of volume, rising the concentration of nucleation centers.[49] The potentiality to produce and control metallic nanoparticles within complex microstructures is illustrated in the inset of Figure 7, in which a butterfly of Au NPs was designed. It is important to note that in this example two steps were applied: (*i*) fs-laser micromachining and (*ii*) heat

treatment. As mentioned before, if a high repetition laser had been employed the second step could be ruled out. We have reported the differences concerning the usage of kHz or MHz laser systems for the space-selective formation of silver and copper NPs in borosilicate glass.[52] Basically, multiphoton absorption and ionization, caused by fs-laser exposure, lead to free electron generation and photoreduction reactions. When kHz repetition rate laser is applied, such effects are observed in the absorption spectrum through color centers, defects and other induced electronic states. Then, this preferential light absorption gives rise to the plasmon band after the suitable annealing. On the other hand, metallic nanoparticles readily precipitate when thermal effects associated with high repletion rates are presents, and the SPR band is observed even without heat treatment. An detailed study about the ionic species and clusters of silver induced by femtosecond laser was recently reported.[53]

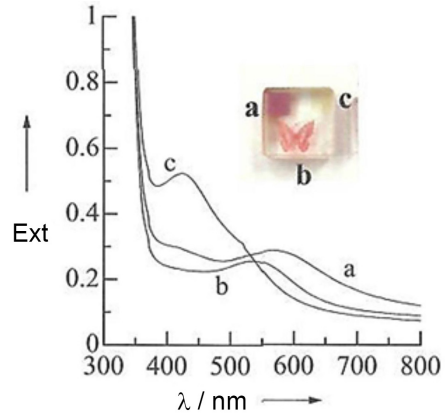

Figure 7. Extinction spectra of Au_2O_3 doped silicate glass irradiated with fs-laser beam of (a) 6.5×10^{13} W cm^{-2}; (b) 2.3×10^{14} W cm^{-2}; (c) 5.0×10^{16} W cm^{-2} and further annealed at 550 ºC during 1 h. The inset shows the picture of this sample and the corresponding irradiated areas (adapted from reference 49).

Metallic nanoparticles have been exploited for improvement of the nonlinear optical properties in different material systems.[54] Naturally, not only the optical nonlinearities but also linear optical properties are affected by SPR. An increase of the refractive index of 4.6% (or $\Delta n = 7 \times 10^{-2}$) has been reported due to the presence of silver NPs in silicate glasses.[51] Thus, the precipitation of Ag NPs using fs-laser micromachining improves the refractive index changes caused by nonlinear interactions and additionally incorporates the optical properties associated with the metallic nanoparticle in the microstructure. Figure 8 displays a 3D-waveguide containing metallic silver nanoparticles in its core, produced by femtosecond laser irradiation in phosphate glass.[16] The waveguide size can be increased from 2 to 30 μm, while its propagation loss decreases from 1.4 to 0.5 dB mm^{-1} at 632.8 nm, according to the increase of the pulse energy (37-60 nJ). It was found a dependency of light intensity profile with the region of NP precipitation, which may result in a non-uniform Δn distribution and therefore additional losses. Nonetheless, all benefits related to Ag NPs, like short lifetimes, high quantum yield and stability against photobleaching,[55] are integrated in the waveguide, bringing new prospects for the development of all-optical devices. For instance, 2D and 3D nonlinear architectures with second harmonic generation has been demonstrated.[56]

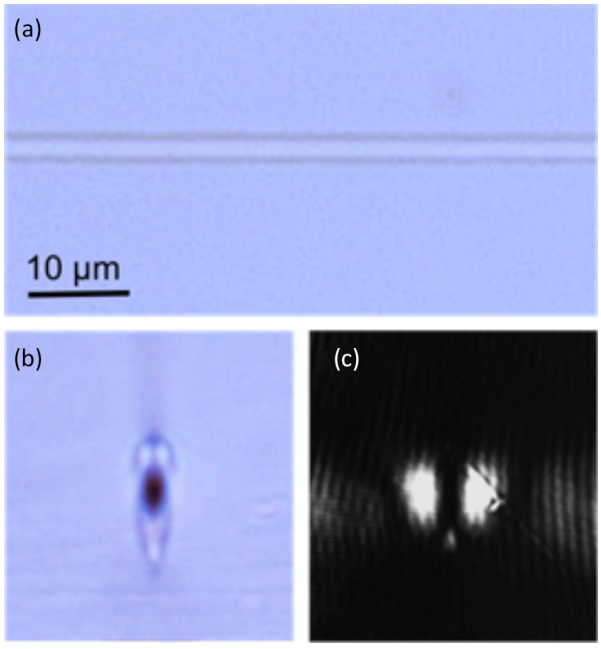

Figure 8. Optical microscopy images of the waveguide fabricated in glass by direct laser write, using only single pass of an oscillator fs-laser (800 nm, 50 fs and 5 MHz of repetition rate); (a) top view; (b) end views; (c) displays the near-field output profile of the light guided at 632.8 nm.[16] Reprinted with permission from (Almeida *et al.*,[16] 2014). Copyright (2015), AIP Publishing LLC.

We have discussed the effects of longitudinal and transversal laser write as well as the influence of repetition rate over the fabrication of waveguides in glass. Among the experimental parameters, pulse duration also affects the laser-induced damage in transparent materials. Experiments and modeling on fused silica are studied,[57,58] for regimes of short and ultra-short pulses respectively, in which contributions from multiphoton, tunnel, impact and avalanche ionizations are thoroughly described. Also investigating fused silica, Mazur group found a dependence of NA with the damage caused by fs-laser pulses.[59] For NA ≥ 0.10 there is a sharp threshold energy that indicates the onset of multiphoton ionization. Such threshold energy is well below the critical power for self-focusing for a regime of high NA (greater than 0.25), resulting in structures that matches with the confocal

parameter, whereas lower NAs cause broken filaments, suggesting multiple refocusing of the femtosecond laser beam.[59,60]

Most of the key works concerning laser-induced damage and waveguides are performed using standard or commercial glasses. Nevertheless, studies on optical nonlinearities, addressed in the former section, demonstrate the importance of tailoring material properties through the composition, stimulating the usage multicomponent glass for direct laser write. For instance, quantitative measurements on fs-laser induced Δn have shown strong dependency on glasses composition, its structure and thermal properties.[11,61] Positives, negatives and nonuniform variations result not only from the glass composition but also from the laser writing parameters.[62] The waveguide shape is also affected by composition, as in the case of heavy metal oxide glasses, which have high $n_2$and hence self-focusing effect.[63] Even so, Y-splitters, directional couplers, supercontinuum and second harmonic generation have been demonstrated in those glasses using fs-laser micromachining.[64] In addition, heavy metal oxide glasses are excellent hosts for earth-rare elements, enabling the development of active waveguides with internal gain in the C-band.[65]

5. Final Remarks

In this paper we presented a survey of results obtained by our and other research groups on the study of the nonlinear refraction and absorption in special glasses, as well as on the processing of such materials by femtosecond laser pulses. From the point of view of nonlinear spectroscopy, very interesting results have been obtained, revealing a clear interdependence between the glass composition and the nonlinear refraction and absorption that can lead to tailoring the material's optical properties for applications in optics and photonics. Considering the processing of such special glasses, the results here compiled demonstrate that femtosecond laser is a powerful tool to change glassy materials properties by micromachining, which led to obtaining, among other applications, the waveguide fabrication and the controlled production of metallic nanoparticles. Therefore, those two research areas combined, nonlinear spectroscopy and fs-laser micromachining, allows exploiting new venues into the use of special glasses for the development of devices.

Acknowledgements

The authors would like to acknowledge the support from FAPESP (Fundação de Amparo à Pesquisa do Estado de São Paulo), CNPq (Conselho Nacional de Desenvolvimento Científico e Tecnológico), CAPES (Coordenação de Aperfeiçoamento de Pessoal de Nível Superior), the Air Force Office of Scientific Research, and interaction with previous students and collaborators.

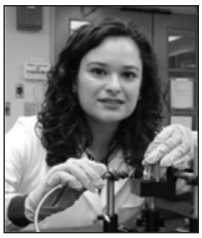

Juliana M. P. Almeida *received her BSc in Natural Science with emphasis in Physics from University of São Paulo (USP) in 2009. She concluded her master in Materials Science and Engineering two years later at USP and then enrolled in the same PhD program. Nowadays, she is a senior PhD student working on third-optical nonlinearities of heavy metal oxide glass, as well as fs-laser micromachining for the development of 3D waveguides. During her one year internship at Princeton University (2013-2014) she could extend her research to amorphous chalcogenides focusing on the synthesis of metamaterials for mid-infrared.*

Gustavo F. B. Almeida *received the Bachelor's and Master's degrees in Physics both from the University of São Paulo, São Carlos, Brazil, in 2011 and 2014, respectively. He is currently working toward the Doctorate degree at the São Carlos Institute of Physics, University of São Paulo. His research interest is focused on the micromachining of organic and inorganic materials using femtosecond lasers and its applications.*

Leonardo De Boni *received his PhD in Physics in 2004 from University of São Paulo (USP), Brazil. In 2005 he worked as a postdoctoral researcher at University of São Paulo (USP) and 2007 as a postdoctoral at Chemistry Department at University of Central Florida, USA. In 2010 he joined São Carlos Institute of Physics at USP as Physicist, and became Assistant Professor in 2014. From his PhD to nowadays he worked on nonlinear optics, nonlinear spectroscopy and ultrafast dynamics.*

Cleber R. Mendonça *received his PhD in Physics in 2000 from University of São Paulo (USP), Brazil. In 2001 he worked as a postdoctoral research at The College of Optics and Photonics (CREOL), USA. He joined São Carlos Institute of Physics at USP in 2001, where he currently is a*

Full Professor. From 2005-2007 he worked on fs-laser microfabrication and ultrafast dynamics as a visiting Scientist at Harvard University. He received the ICO/ICTP Gallieno Denardo Award in 2010 and was designed OSA Senior member in 2013. His current research interests are nonlinear optical processes and fs-laser microfabrication.

References

1. Brow, R. K.; *J. Non-Cryst. Solids* **2000**, *263*, 1.
2. El-Mallawany, R. A. H.; *Tellurite Glasses Handbook: Physical Properties and Data*; CRC Press: Boca Raton, FL, 2002.
3. Yamane, M.; Asahara, Y.; *Glasses for Photonics*; Cambridge University Press: Port Chester, New York, 2000.
4. Campbell, J. H.; Suratwala, T. I.; *J. Non-Cryst. Solids* **2000**, *263*, 318; Poirier, G.; Ottoboni, F. S.; Cassanjes, F. C.; Remonte, A.; Messaddeq, Y.; Ribeiro, S. J. L.; *J. Phys. Chem. B* **2008**, *112*, 4481.
5. Sekhar, H.; Kiran, P. P.; Rao, D. N.; *Mater. Chem. Phys.* **2011**, *130*, 113.
6. Smolorz, S.; Kang, I.; Wise, F.; Aitken, B. G.; Borrelli, N. F.; *J. Non-Cryst.* Solids **1999**, *256*, 310.
7. Inouye, H.; Tanaka, K.; Tanahashi, I.; Hirao, K.; *Phys. Rev. B* **1998**, *57*, 11334.
8. Kowalevicz, A. M.; Sharma, V.; Ippen, E. P.; Fujimoto, J. G.; Minoshima, K.; *Opt. Lett.* **2005**, *30*, 1060; Li, Y.; Yamada, K.; Ishizuka, T.; Watanabe, W.; Itoh, K.; Zhou, Z. X.; *Opt. Express* **2002**, *10*, 1173; Correa, D. S.; Cardoso, M. R.; Tribuzi, V.; Misoguti, L.; Mendonca, C. R.; *IEEE J. Sel. Top. Quantum Electron.* **2012**, *18*, 176.
9. Gattass, R. R.; Mazur, E.; *Nat. Photonics* **2008**, *2*, 219.
10. Minoshima, K.; Kowalevicz, A. M.; Hartl, I.; Ippen, E. P.; Fujimoto, J. G.; *Opt. Lett.* **2001**, *26*, 1516; Nolte, S.; Will, M.; Burghoff, J.; Tuennermann, A.; *Appl. Phys. A* **2003**, *77*, 109; Glezer, E. N.; Milosavljevic, M.; Huang, L.; Finlay, R. J.; Her, T. H.; Callan, J. P.; Mazur, E.; *Opt. Lett.* **1996**, *21*, 2023; Streltsov, A. M.; Borrelli, N. F.; *Opt. Lett.* **2001**, *26*, 42.
11. Davis, K. M.; Miura, K.; Sugimoto, N.; Hirao, K.; *Opt. Lett.* **1996**, *21*, 1729.
12. Miura, K.; Qiu, J. R.; Inouye, H.; Mitsuyu, T.; Hirao, K.; *Appl. Phys. Lett.* **1997**, *71*, 3329.
13. Schaffer, C. B.; Brodeur, A.; Garcia, J. F.; Mazur, E.; *Opt. Lett.* **2001**, *26*, 93.
14. Krol, D. M.; *J. Non-Cryst. Solids* **2008**, *354*, 416.
15. Royon, A.; Petit, Y.; Papon, G.; Richardson, M.; Canioni, L.; *Opt. Mater. Express* **2011**, *1*, 866.
16. Almeida, J. M. P.; Ferreira, P. H. D.; Manzani, D.; Napoli, M.; Ribeiro, S. J. L.; Mendonca, C. R.; *J. Appl. Phys.* **2014**, *115*, 193507.
17. Sheikbahae, M.; Said, A. A.; van Stryland, E. W.; *Opt. Lett.* **1989**, *14*, 955; Sheikbahae, M.; Said, A. A.; Wei, T. H.; Hagan, D. J.; van Stryland, E. W.; IEEE *J. Sel. Top. Quantum Electron.* **1990**, *26*, 760.
18. de Boni, L.; Andrade, A. A.; Misoguti, L.; Mendonca, C. R.; Zilio, S. C.; *Opt. Express* **2004**, *12*, 3921.
19. Almeida, J. M. P.; de Boni, L.; Avansi, W.; Ribeiro, C.; Longo, E.; Hernandes, A. C.; Mendonca, C. R.; *Opt. Express* **2012**, *20*, 15106.
20. Almeida, J. M. P.; de Boni, L.; Hernandes, A. C.; Mendonca, C. R.; *Opt. Express* **2011**, *19*, 17220.
21. Sowa, S.; Watanabe, W.; Tamaki, T.; Nishii, J.; Itoh, K.; *Opt. Express* **2006**, *14*, 291.
22. Friberg, S. R.; Smith, P. W.; *IEEE J. Quantum Electron.* **1987**, *23*, 2089.
23. Thomazeau, I.; Etchepare, J.; Grillon, G.; Migus, A.; *Opt. Lett.* **1985**, *10*, 223.
24. Smith, P. W.; Tomlinson, W. J.; Eilenberger, D. J.; Maloney, P. J.; *Opt. Lett.* **1981**, *6*, 581.
25. Hall, D. W.; Newhouse, M. A.; Borrelli, N. F.; Dumbaugh, W. H.; Weidman, D. L.; *Appl. Phys. Lett.* **1989**, *54*, 1293.
26. Zakery, A.; Elliott, S. R.; *J. Non-Cryst. Solids* **2003**, *330*, 1.
27. Vogel, E. M.; Kosinski, S. G.; Krol, D. M.; Jackel, J. L.; Friberg, S. R.; Oliver, M. K.; Powers, J. D.; *J. Non-Cryst. Solids* **1989**, *107*, 244.
28. Lines, M. E.; *J. Appl. Phys.* **1991**, *69*, 6876.
29. Sabadel, J. C.; Armand, P.; Cachau-Herreillat, D.; Baldeck, P.; Doclot, O.; Ibanez, A.; Philippot, E.; *J. Solid State Chem.* **1997**, *132*, 411.
30. Milam, D.; *Appl. Opt.* **1998**, *37*, 546.
31. Almeida, J. M. P.; Fonseca, R. D.; de Boni, L.; Diniz, A. R. S.; Hernandes, A. C.; Ferreira, P. H. D.; Mendonca, C. R.; *Opt. Mater.* **2015**, *42*, 522.
32. Uchida, K.; Kaneko, S.; Omi, S.; Hata, C.; Tanji, H.; Asahara, Y.; Ikushima, A. J.; Tokizaki, T.; Nakamura, A.; *J. Opt. Soc. Am. B: Opt. Phys.* **1994**, *11*, 1236.
33. Falcão-Filho, E. L.; Bosco, C. A. C.; Maciel, G. S.; Acioli, L. H.; de Araújo, C. B.; Lipovskii, A. A.; Tagantsev, D. K.; *Phys. Rev. B* **2004**, *69*, 134204.
34. de Boni, L.; Barbano, E. C.; de Assumpcao, T. A.; Misoguti, L.; Kassab, L. R. P.; Zilio, S. C.; *Opt. Express* **2012**, *20*, 6844.
35. Manzani, D.; Almeida, J. M. P.; Napoli, M.; de Boni, L.; Nalin, M.; Afonso, C. R. M.; Ribeiro, S. J. L.; Mendonça, C. R.; *Plasmonics* **2013**, *8*, 1167.
36. Almeida, J. M. P.; da Silva, D. S.; Kassab, L. R. P.; Zilio, S. C.; Mendonca, C. R.; de Boni, L.; *Opt. Mater*. **2014**, *36*, 829.
37. Qu, S. L.; Gao, Y. C.; Jiang, X. W.; Zeng, H. D.; Song, Y. L.; Qiu, H. R.; Zhu, C. S.; Hirao, K.; *Opt. Commun.* **2003**, *224*, 321.
38. Du, D.; Liu, X.; Korn, G.; Squier, J.; Mourou, G.; *Appl. Phys. Lett.* **1994**, *64*, 3071.

39. Hirao, K.; Miura, K.; *J. Non-Cryst. Solids* **1998**, *239*, 91.
40. Ponader, C. W.; Schroeder, J. F.; Streltsov, A. M.; *J. Appl. Phys.* **2008**, *103*, 063516.
41. Will, M.; Nolte, S.; Chichkov, B. N.; Tunnermann, A.; *Appl. Opt.* **2002**, *41*, 4360.
42. Osellame, R.; Taccheo, S.; Marangoni, M.; Ramponi, R.; Laporta, P.; Polli, D.; de Silvestri, S.; Cerullo, G.; *J. Opt. Soc. Am. B* **2003**, *20*, 1559; Cerullo, G.; Osellame, R.; Taccheo, S.; Marangoni, M.; Polli, D.; Ramponi, R.; Laporta, P.; de Silvestri, S.; *Opt. Lett.* **2002**, *27*, 1938.
43. Ams, M.; Marshall, G. D.; Spence, D. J.; Withford, M. J.; *Opt. Express* **2005**, *13*, 5676.
44. Cheng, Y.; Sugioka, K.; Midorikawa, K.; Masuda, M.; Toyoda, K.; Kawachi, M.; Shihoyama, K.; *Opt. Lett.* **2003**, *28*, 55.
45. Cerami, L. R.; Mazur, E.; Nolte, S.; Schaffer, C. B. In *Ultrafast Optics*; Trebino, R.; Squier, J., eds.; Trafford Publishing: Victoria, 2007.
46. Eaton, S. M.; Zhang, H. B.; Herman, P. R.; *Opt. Express* **2005**, *13*, 4708.
47. Sakakura, M.; Shimizu, M.; Shimotsuma, Y.; Miura, K.; Hirao, K.; *Appl. Phys. Lett*. **2008**, *93*, 3433.
48. Kanehira, S.; Miura, K.; Hirao, K.; *Appl. Phys. Lett.* **2008**, *93*, 023112; Miura, K.; Qiu, J. R.; Mitsuyu, T.; Hirao, K.; *Opt. Lett.* **2000**, *25*, 408.
49. Qiu, J. R.; Jiang, X. W.; Zhu, C. S.; Shirai, M.; Si, J.; Jiang, N.; Hirao, K.; *Angew. Chem. Int. Ed.* **2004**, *43*, 2230.
50. Shin, J.; Jang, K.; Lim, K.; Sohn, I.; Noh, Y.; Lee, J.; *Appl. Phys. A* **2008**, *93*, 923; Teng, Y.; Zhou, J.; Luo, F.; Lin, G.; Qiu, J.; *J. Non-Cryst. Solids* **2011**, *357*, 2380; Shimotsuma, Y.; Hirao, K.; Kazansky, P. G.; Qiu, H. R.; *Jpn. J. Appl. Phys., Part 1* **2005**, *44*, 4735.
51. Dai, Y.; Yu, G.; He, M.; Ma, H.; Yan, X.; Ma, G.; *Appl. Phys. B: Lasers Opt.* **2011**, *103*, 663.
52. Almeida, J. M. P.; Tribuzi, V.; Fonseca, R. D.; Otuka, A. J. G.; Ferreira, P. H. D.; Mastelaro, V. R.; Brajato, P.; Hernandes, A. C.; Dev, A.; Voss, T.; Correa, D. S.; Mendonca, C. R.; *Opt. Mater.* **2013**, *35*, 2643.
53. Marquestaut, N.; Petit, Y.; Royon, A.; Mounaix, P.; Cardinal, T.; Canioni, L.; *Adv. Funct. Mater.* **2014**, *24*, 5824.
54. Fukumi, K.; Chayahara, A.; Kadono, K.; Sakaguchi, T.; Horino, Y.; Miya, M.; Fujii, K.; Hayakawa, J.; Satou, M.; *J. Appl. Phys.* **1994**, *75*, 3075; Tokizaki, T.; Nakamura, A.; Kaneko, S.; Uchida, K.; Omi, S.; Tanji, H.; Asahara, Y.; *Appl. Phys. Lett.* **1994**, *65*, 941; Tanahashi, I.; Manabe, Y.; Tohda, T.; Sasaki, S.; Nakamura, A.; *J. Appl. Phys.* **1996**, *79*, 1244.
55. Diez, I.; Ras, R. H. A.; *Nanoscale* **2011**, *3*, 1963.
56. Papon, G.; Marquestaut, N.; Petit, Y.; Royon, A.; Dussauze, M.; Rodriguez, V.; Cardinal, T.; Canioni, L.; *J. Appl. Phys.* **2014**, *115*, 113103; Mishchik, K.; Petit, Y.; Brasselet, E.; Royon, A.; Cardinal, T.; Canioni, L.; *Opt. Lett.* **2015**, *40*, 201.
57. Tien, A. C.; Backus, S.; Kapteyn, H.; Murnane, M.; Mourou, G.; *Phys. Rev. Lett.* **1999**, *82*, 3883.
58. Chimier, B.; Uteza, O.; Sanner, N.; Sentis, M.; Itina, T.; Lassonde, P.; Legare, F.; Vidal, F.; Kieffer, J. C.; *Phys. Rev. B* **2011**, *84*, 094104.
59. Ashcom, J. B.; Gattass, R. R.; Schaffer, C. B.; Mazur, E.; *J. Opt. Soc. Am. B* **2006**, *23*, 2317.
60. Nguyen, N. T.; Saliminia, A.; Liu, W.; Chin, S. L.; Vallee, R.; *Opt. Lett.* **2003**, *28*, 1591.
61. Fletcher, L. B.; Witcher, J. J.; Troy, N.; Reis, S. T.; Brow, R. K.; Krol, D. M.; *Opt. Express* **2011**, *19*, 7929.
62. Bhardwaj, V. R.; Simova, E.; Corkum, P. B.; Rayner, D. M.; Hnatovsky, C.; Taylor, R. S.; Schreder, B.; Kluge, M.; Zimmer, J.; *J. Appl. Phys.* **2005**, *97*, 121109; Chan, J. W.; Huser, T. R.; Risbud, S. H.; Hayden, J. S.; Krol, D. M.; *Appl. Phys. Lett.* **2003**, *82*, 2371.
63. Siegel, J.; Fernandez-Navarro, J. M.; Garcia-Navarro, A.; Diez-Blanco, V.; Sanz, O.; Solis, J.; Vega, F.; Armengol, J.; *Appl. Phys. Lett.* **2005**, *86*, 121109, 1.
64. Yang, W.; Corbari, C.; Kazansky, P. G.; Sakaguchi, K.; Carvalho, I. C. S.; *Opt. Express* **2008**, *16*, 16215.
65. Fernandez, T. T.; Valle, G. D.; Osellame, R.; Jose, G.; Chiodo, N.; Jha, A.; Laporta, P.; *Opt. Express* **2008**, *16*, 15198; Silva, D. M.; Kassab, L. R. P.; Olivero, M.; Lemos, T. B. N.; Silva, D. V.; Gomes, A. S. L.; *Opt. Mater.* **2011**, *33*, 1902.

Submitted: June 14, 2015
Published online: September 15, 2015

FAPESP has sponsored the publication of this article.